Calculations of Ignition Lags for Methane-Air Mixtures by Chemical Kinetics

N.Miyamoto, H.Ogawa and K.Doi

Department of Mechanical Engineering
Hokkaido University
N-13, W-8, Sapporo 060
Japan

ABSTRACT

One of the major alternative fuels, methane, is of increasing interest for use in internal combustion engines.

In this paper, precise and time-efficient calculations of ignition lags and oxidation processes in a wide range of methane-air mixtures were determined with a comparatively small number of chemical kinetic reactions in the usual combustion range of internal combustion engines.

The influences of each chemical reaction on time-resolved species concentrations were also determined. A specific concentration of OH radicals resulted in the onset of spark knocking or autoignition in a spark ignition engine, almost independent on engine operating conditions such as spark timing, compression ratio, or equivalence ratio.

As a result, autoignition and ignition lags can be predicted precisely and easily by focusing on the concentration of OH radicals calculated with the chemical kinetic reactions.

INTRODUCTION

World reserves of crude oil are being depleted rapidly, creating incentives for promotion and further evaluation of alternative fuel sources for internal combustion engines. One such alternative fuel is natural gas with the primary component methane CH_4.

A better understanding of its ignition and oxidation characteristics is necessary, and one concern is knocking problems in higher compression ratio spark ignition engines and duel fuel diesel engines with natural gas, LNG, and CNG.

Research on methane oxidation reactions may be divided into two categories. One is basic research on the chemical kinetic reactions of methane, determining the probabilities of various elementary reactions of chemical species(1)-(10). Some researches have used the shock tube to optically determine some of the elementary reactions involved.

The other category of research, which is closely related to this investigation, is the applied research on methane kinetic reactions, including analyses of burning rates, autoignition, and combustion products of methane-air mixtures(11)-(14). For example, Karim et al. have investigated autoignition phenomena especially in diesel engines with diesel fuel as the main fuel and induced methane as the auxiliary fuel. Considerable amounts of induced methane tended to cause more knocking in diesel engines, and also in spark ignition engines with higher compression ratios, higher intake air temperatures, and advanced spark timings. Karim et al. also proposed a chemical model of knocking with 32 chemical reactions for lean methane mixtures in duel fuel diesel engines(14).

Performance and exhaust gas emission of diesel engines with methane induction from the intake manifold have long been investigated(13)-(15). Methane induction increases NOx, noise, HC emissions, but decreases brake specific fuel consumption and soot emission.

In this investigation, more precise and efficient calculations of ignition lags and oxidation processes for a wide range of methane-air mixtures were established with a lower number of chemical reactions in internal combustion engines. Only 16 predominant chemical reactions among 31, were selected and found to be sufficient for precise calculations of ignition lags and oxidation processes of the methane-air mixtures.

A critical concentration of OH radical was found to be a determinant in autoignition or knocking in spark ignition engines.

CALCULATION OF IGNITION LAGS WITH CHEMICAL KINETICS

Reaction systems with NS species and NR chemical reactions are assumed for methane-air mixtures. Putting A_i as the i-th chemical species among NS species and ν_{ij} as the stoichiometric coefficient for A_i in the j-th equation of the NR equations. The j-th reaction equation in Table 1 can be generally described as the homogeneous equation:

$$\nu_{1j}A_1+\nu_{2j}A_2+\cdots+\nu_{ij}A_i+\cdots+\nu_{NSj}A_{NS}=0 \qquad [1]$$

where: ν_{ij} is negative for reacting compounds of A_i and positive for produced compounds.

Also, setting k_{jf} as the reaction rate coefficient for dispersion of A_i, and k_{jr} as that for production of A_i, the reaction rate of A_i, $\frac{d[A_i]}{dt}$, in a reaction system becomes as follow:

Table 1 The chemical reactions considered and their reaction rates

$k_f = FRC \cdot T^{FRP} \cdot \exp(-FRX/RT)$

$k_r = RRC \cdot T^{RRP} \cdot \exp(-RRX/RT)$

	Chemical Reaction	FRC	FRP	FRX	RRC	RRP	RRX	REF
1.	$CH_4=CH_3+H$	1.400D+17	0.0	8.840D+4	2.840D+11	1.00	-1.951D+4	1
2.	$CH_4+OH=CH_3+H_2O$	3.000D+13	0.0	6.000D+3	4.972D+12	0.0	2.068D+4	2
3.	$CH_4+H=CH_3+H_2$	1.250D+14	0.0	1.190D+4	4.800D+12	0.0	1.143D+4	1
4.	$CH_4+O=CH_3+OH$	2.000D+13	0.0	9.200D+3	3.340D+11	0.0	6.640D+3	1
5.	$CH_3+O_2=CH_2O+OH$	6.920D+11	0.0	4.530D+3	7.210D+11	0.0	5.805D+4	1
6.	$CH_3+OH=CH_2O+H_2$	4.000D+12	0.0	0.0	1.200D+14	0.0	7.172D+4	1
7.	$CH_3+O=CH_2O+H$	1.300D+14	0.0	2.000D+3	1.700D+15	0.0	7.163D+4	1
8.	$CH_2O+OH=CHO+H_2O$	5.400D+14	0.0	6.300D+3	1.870D+14	0.0	3.612D+4	1
9.	$CH_2O+O=CHO+OH$	5.000D+13	0.0	4.600D+3	1.750D+12	0.0	1.717D+4	1
10.	$CH_2O+H=CHO+H_2$	1.350D+13	0.0	3.760D+3	1.070D+12	0.0	1.843D+4	1
11.	$CHO+OH=CO+H_2O$	1.000D+14	0.0	0.0	2.800D+15	0.0	1.051D+5	1
12.	$CHO+H=CO+H_2$	3.000D+10	1.00	0.0	1.970D+11	1.00	9.000D+4	3
13.	$CHO+O=CO+OH$	1.000D+14	0.0	0.0	2.880D+14	0.0	8.790D+4	1
14.	$CO+O=CO_2$	5.900D+15	0.0	4.100D+3	5.500D+21	-1.00	1.318D+5	1
15.	$CO+OH=CO_2+H$	1.500D+07	1.30	-7.650D+2	1.680D+09	1.30	2.157D+4	1
16.	$CO+O_2=CO_2+O$	3.140D+11	0.0	3.760D+4	2.780D+12	0.0	4.383D+4	1
17.	$H+O_2=O+OH$	2.200D+14	0.0	1.679D+4	1.740D+13	0.0	6.770D+2	1
18.	$H_2O=H+OH$	7.420D+28	-3.00	1.226D+5	2.200D+22	-2.00	0.0	4
19.	$O+H=OH$	1.000D+16	0.0	0.0	8.000D+16	-1.00	1.037D+5	1
20.	$H_2=H+H$	7.790D+23	-2.00	1.074D+5	1.000D+18	-1.00	0.0	5
21.	$H_2O+O=OH+OH$	6.800D+13	0.0	1.835D+4	6.300D+12	0.0	1.100D+3	1
22.	$O+O=O_2$	4.700D+15	-0.28	0.0	5.100D+15	0.0	1.150D+5	1
23.	$H_2+O=H+OH$	1.800D+10	1.00	8.900D+3	8.300D+09	1.00	6.950D+3	1
24.	$H_2+OH=H_2O+H$	2.200D+13	0.0	5.150D+3	9.520D+13	0.0	2.030D+4	4
25.	$O+N_2=NO+N$	7.600D+13	0.0	7.554D+4	1.600D+13	0.0	0.0	1
26.	$NO+O=N+O_2$	2.097D+09	1.00	3.856D+4	9.810D+09	1.00	6.610D+3	6
27.	$N+OH=NO+H$	9.620D+13	0.0	7.350D+2	2.600D+14	0.0	4.880D+4	1
28.	$N+N=N_2$	2.970D+17	-0.99	0.0	1.246D+24	-1.99	2.286D+5	6
29.	$NO=N+O$	4.000D+20	-1.50	1.510D+5	2.500D+19	-1.33	0.0	1
30.	$CH_3+CHO=CH_4+CO$	3.000D+11	0.50	0.0	5.140D+13	0.50	9.047D+4	1
31.	$CH_3+CH_2O=CH_4+CHO$	1.000D+10	0.50	6.000D+3	2.090D+10	0.50	2.114D+4	1
				(cal/mol)			(cal/mol)	

$$\frac{d[A_i]}{dt} = \sum_j^{NR} \left(\nu_{ij} \left(k_{jf} \bar{\prod_i^{NS}} [A_i]^{|\nu_{ij}|} - k_{jr} \dot{\prod_i^{NS}} [A_i]^{|\nu_{ij}|} \right) \right) \quad [2]$$

where: $\bar{\prod}$ means multiplying the concentrations of every species $[A_i]$ with negative stoichiometric coefficients.

$\dot{\prod}$ means multiplying the concentrations of every species $[A_i]$ with positive stoichiometric coefficients.

The 31 chemical reactions shown in Table 1 are evaluated and discussed in this paper, and for 31 reaction equations, the number of species, NS, is 15: CH_4, CH_3, CH_2O, CHO, CO, CO_2, H_2O, H_2, O_2, OH, H, O, N_2, NO, and N.

Reaction rates for each chemical species were calculated numerically with Gear's method. Adiabatic temperatures were also calculated with enthalpy changes of each chemical reaction using the specific heats(1).

First the calculation time interval was determined as shown in Fig. 1. The abscissa is the OH radical concentration 1 μs after the beginning of the oxidation for different initial gas temperatures. As shown in the figure, the OH radical concentration abruptly decreases or cannot be calculated correctly beyond specific time intervals, above 1300 K of initial temperature with the 10^{-7}s internal, and above 1600 K with the 10^{-8}s interval. The shorter time intervals were necessary for precise calculations of each species at higher initial temperatures. These results indicate that time intervals shorter than 10^{-11}s are adequate for precise calculation of oxidation processes in the usual range of initial temperatures.

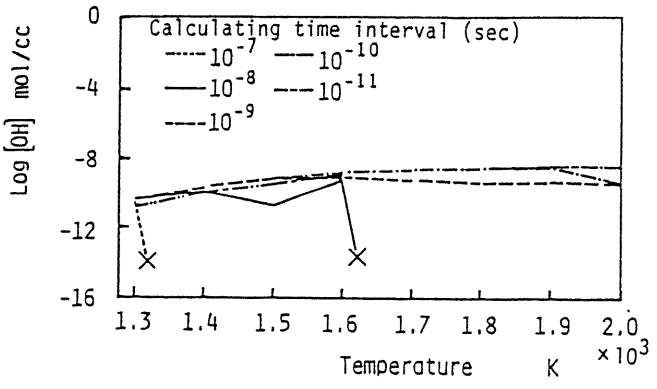

Fig. 1 Effect of calculation time intervals on OH radical concentrations
[ϕ=1.0, 0.1 MPa, 16 reactions]

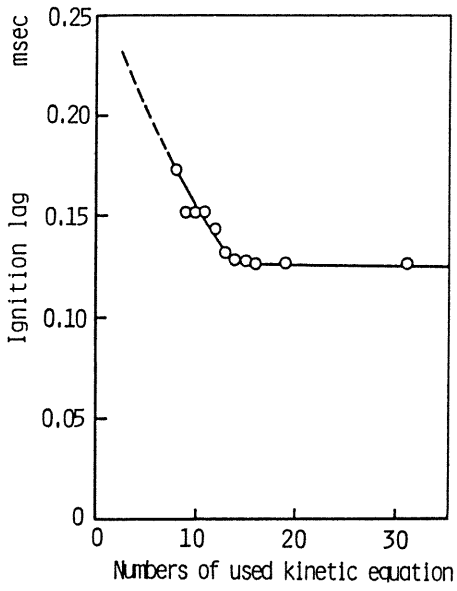

Fig. 2 Relation between calculated ignition lags and number of chemical kinetic reactions in the calculations
[1500 K, ϕ=1.0, 0.1 MPa]

Calculation of ignition lags requires a determination or definition of the ignition point in the oxidation processes. By examining the different chemical species over a wide range of combustion conditions, the OH radical concentration was found to be a good determinant for ignition. Higgins has also reported that OH radical concentration is a reasonable determinant for ignition(16).

In this paper, an OH concentration of 10^{-8} mol/cc was used to the calculate ignition lags. The ignition lags did not show large differences when the OH radical concentration varied by one order of magnitude (10^{-8} mol/cc and 10^{-9} mol/cc).

A small number of chemical reactions is desirable to be able to calculate ignition lags and oxidation processes in a short time. Fig. 2 shows the relation between the number of kinetic equations and ignition lags with methane-air mixtures under the initial temperatures of 1500 K. The number of equations and the equations included in the calculation of ignition lags are shown in

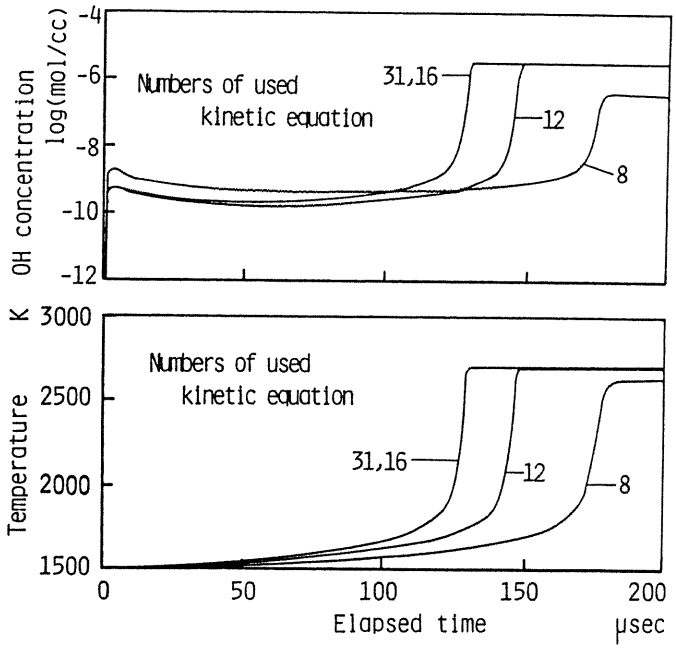

Fig. 3 Effect of number of kinetic reactions on time-resolved OH radical concentrations
[1500 K, ϕ=1.0, 0.1 MPa]

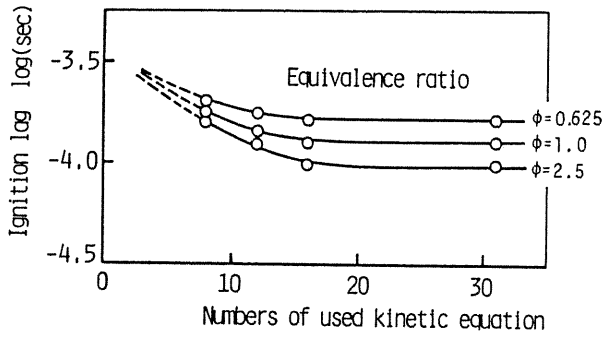

Fig. 4 Number of kinetic reactions and calculated ignition lags in some equivalence ratios
[1500 K, 0.1 MPa]

Table 2. The figure shows that a decrease in the number of kinetic equations from 31 to about 16 does not change the ignition lags, and that a further decrease in number of equations increase the ignition lags significantly. The time-resolved OH radical concentrations and temperatures after the start of oxidation of methane can be seen in Fig. 3 where the number of kinetic equations are shown as parameters. The increase in ignition lags calculated with fewer than 16 kinetic reactions becomes clear from this figure, which shows that the elapsed time when OH radical and temperature tend to increase rapidly are remarkable retarded especially for less than 16 equations.

The qualitative relation between ignition lags and number of kinetic equations did not change when oxidation conditions such as initial temperature, pressure, or equivalence ratio were changed. The relation between ignition lags and the number of equations under different equivalence ratios are shown in Fig. 4.

Table 2 Groups of chemical reactions for calculations

No	Chemical Reactions	number of kinetic equations involved						
		31	19	16	14	12	10	8
1	$CH_4=CH_3+H$	×	×	×	×	×	×	×
2	$CH_4+OH=CH_3+H_2O$	×	×	×	×	×		
3	$CH_4+H=CH_3+H_2$	×	×	×	×			
4	$CH_4+O=CH_3+OH$	×	×	×				
5	$CH_3+O_2=CH_2O+OH$	×	×	×	×	×	×	×
6	$CH_3+OH=CH_2O+H_2$	×	×	×	×	×	×	×
7	$CH_3+O=CH_2O+H$	×	×					
8	$CH_2O+OH=CHO+H_2O$	×	×	×	×	×	×	×
9	$CH_2O+O=CHO+OH$	×						
10	$CH_2O+H=CHO+H_2$	×						
11	$CHO+OH=CO+H_2O$	×	×	×	×	×	×	×
12	$CHO+H=CO+H_2$	×	×	×				
13	$CHO+O=CO+OH$	×						
14	$CO+O=CO_2$	×	×	×	×	×	×	×
15	$CO+OH=CO_2+H$	×						
16	$CO+O_2=CO_2+O$	×						
17	$H+O_2=O+OH$	×	×	×	×	×	×	×
18	$H_2O=H+OH$	×	×	×	×	×	×	×
19	$O+H=OH$	×	×	×	×	×	×	
20	$H_2=H+H$	×	×	×	×	×	×	
21	$H_2O+O=OH+OH$	×	×	×	×	×		
22	$O+O=O_2$	×	×					
23	$H_2+O=H+OH$	×	×					
24	$H_2+OH=H_2O+H$	×						
25	$O+N_2=NO+N$	×						
26	$NO+O=N+O_2$	×						
27	$N+OH=NO+H$	×						
28	$N+N=N_2$	×						
29	$NO=N+O$	×						
30	$CH_3+CHO=CH_4+CO$	×	×	×	×			
31	$CH_3+CH_2O=CH_4+CHO$	×						

Calculating ignition lags and various species with the reduced number of chemical reactions pointed to the principal reactions in methane oxidation. The minimum number of reactions for methane oxidation maybe was eight reactions representing the main oxidation processes from CH_4 to CO_2 and H_2O, as shown in Fig. 5.

Fig. 6 shows the time required for calculation from the beginning till the end of the oxidation processes. As the figure shows, the time required for calculations decreases approximately linearly with the decrease in number of kinetic equations used.

A comparison is made in Fig. 7 between measured ignition lags by shock tube(9),(10) and calculated ones obtained with the 16 chemical reactions on the basis of an OH radical concentration of 10^{-8}mol/cc as the ignition determinator.

The calculated ignition lags appear to be the same or slightly shorter than the measured ones, indicating the adequacy of the method in calculating ignition lags.

EXPERIMENTAL APPARATUS AND PROCEDURES

A single cylinder, water-cooled and naturally aspirated DI diesel engine with a bore x stroke of 96 x 110 mm, was modified to an SI engine with a disc-type combustion chamber and a spark plug at circumference of the chamber. Methane gas was fed to the intake pipe through a gas flow meter. Indicator diagrams were measured with pressure pick-ups installed on the cylinder head. The rates of heat release were calculated from indicator diagrams(18) and used for evaluation of spark knocking.

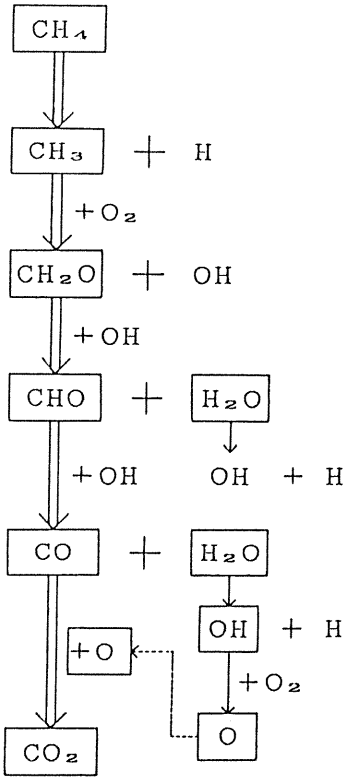

Fig. 5 Main species and intermediate products of the methane-air oxidation process

Spark knocking was investigated under various engine operating conditions at compression ratios of 13-20, spark timings of 25-35°CA BTDC, engine speeds of 800-1200 rpm, and equivalence ratios of 0.65-1.15.

APPLICATION OF CHEMICAL KINETICS ON KNOCKING PHENOMENA IN AN SI ENGINE

Fig. 8 shows an example of indicator diagrams and the rate of heat release(ROHR). In this figure, ROHR from point a to point b results from homogeneous flame propagation. Spark knocking occurs at point b, and then cylinder pressure increases rapidly.

A purpose of this investigation is to predict the onset of knocking and to establish criteria for knocking with the 16 chemical reactions in the end gas of the SI engine. The end gas temperature was calculated with 3-phase model(18) from the actual indicator diagrams. The main concept of the 3-phase model is the energy balance among the three phases of gas in the combustion chamber, the burnt, burning gas, and the gas at the unburnt end. Calculated time-resolved concentrations of some chemical species in the combustion chamber of an SI engine are shown in Fig. 9. The figure shows that concentrations of intermediate products increase up to the point where spark knocking occurs. The determinant for ignition was assumed to be the OH radical concentration, and the OH radical concentration at the point where spark knocking occurs was investigated over a wide range of engine operating conditions, and shown in Fig. 10.

The figure indicates that OH radical concentrations at the point of spark knocking is almost constant at 10^{-10}mol/cc, nearly independent of the engine operating conditions. The operating conditions here include three compression ratios (C.R.), two spark timings (S.T.), five equivalence ratios (ϕ), and three engine speeds (n).

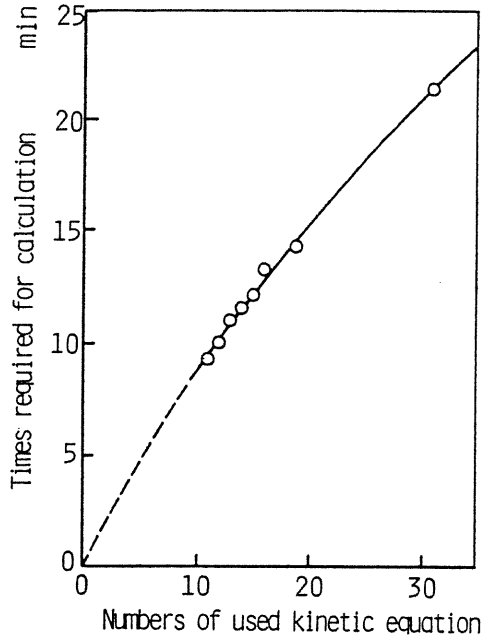

Fig. 6 Time required for calculation and number of chemical kinetic reactions [1500 K, ϕ=1.0, 0.1 MPa]

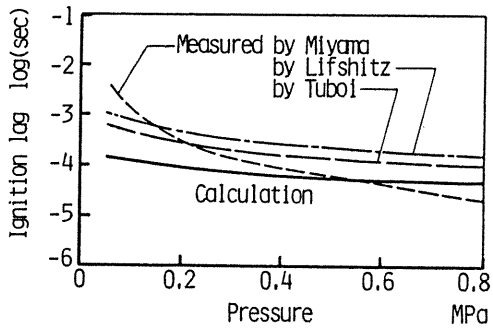

Fig. 7 Comparison between measured and calculated ignition lags [1500K, ϕ=1.0]

The 10^{-10}mol/cc OH concentration at the point of spark knocking in the SI engine seems slightly lower than the 10^{-8}mol/cc which was used in previous section in this paper.

The lower OH radical concentration calculated in the SI engine may be caused by several factors, one of which may be that the calculated end gas temperature did not coincide well with the real end gas temperature. However, the important finding here is not the absolute concentration of OH radicals at the point of spark knocking, but the fact that the OH radical concentration was almost constant over the wide range of engine operating conditions.

In spark ignition engines, prediction of the

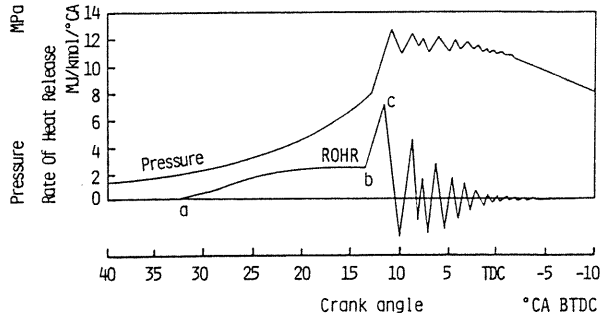

Fig. 8 An indicator diagram and Rate of heat release with spark knocking
[ϕ=0.89, C. R.=16.2, 1200rpm]

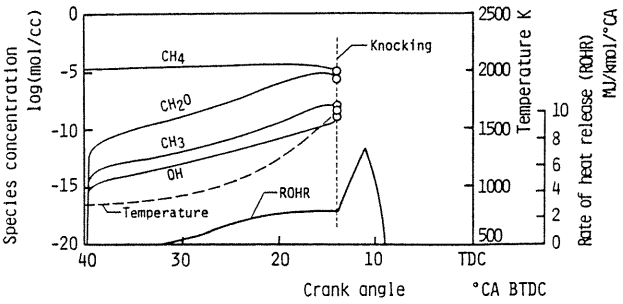

Fig. 9 Time-resolved species up to onset of knocking in a spark ignition engine
[ϕ=0.89, C. R.=16.2, 1200rpm]

propagation of combustion of premixed mixtures is easy today, so that the establishment of the 10^{-10} mol/cc OH radical concentration for ignition or knocking, makes a prediction of spark knocking simply possible from calculations with chemical kinetic reactions.

CONCLUSIONS

The results of this investigation can be summarized as follows;

1. A specific concentration of OH radical, about 10^{-10}mol/cc, calculated with chemical kinetics, gives the onset of spark knocking or autoignition in internal combustion engines, practically independent of the engine operating conditions.

2. Autoignition or ignition lags are simply predicted by the specific concentration of OH radicals calculated with chemical kinetics.

3. Precise and time-efficient calculations of ignition lags and oxidation processes in methane-air mixtures were established with 16 chemical kinetic equations out of 31 equations for methane oxidation reactions.

4. Time intervals required for calculating methane oxidation processes tend to be shorter with higher initial temperatures. A time interval of 10 s is sufficient for calculation of methane oxidation processes in the usual temperature range.

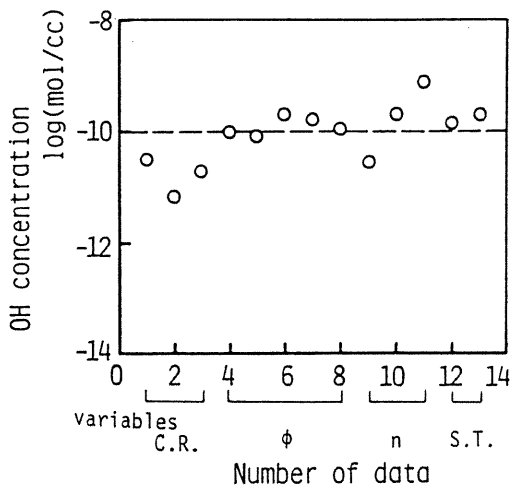

Fig. 10 Calculated OH concentration when spark knocking was determined for a wide range of engine operating conditions

ACKNOWLEDGMENTS

The authors express their appreciations to Mr. I. Ishibashi, Honda Motor Co., and Mr. K. Nakayama, a graduate student at Hokkaido University for their cooperations in this investigation.

REFERENCES

1. C. K. Westbrook, et al., UCID-17833, Lawrence Livermore Lab., 1978.
2. J. Peeters, et al., 14th Int. Symp. on Comb., pp.133, 1978.
3. T. Miyauchi, et al., 16th Int. Symp. on Comb., pp.703, 1977.
4. D. L. Banlch, et al., Evaluated Kinetic Data for High Temperature Reactions, Vol.1-3, 1972-1976, Butterwarths.
5. G. Dixon Lewis, et al., Gas Phase Comb. 1-248, 1977.
6. T. Kuratomi, Bulletin of the Institute of Aviation, Tokyo University, 11, 1975.
7. W. M. Heffington, et al., 16th Int. Symp. on Comb., 997, 1977.
8. C. T. Bowmann, 15th Int. Symp. on Comb., pp.869, 1976.
9. H. Miyama, et al., J. Chem. Phys., pp.40, 1964.
10. T. Tuboi, 15th Int. Symp. on Comb., pp.883, 1976.
11. G. A. Karim, Prog. Energy Comb. Sci. 6, 1980.
12. G. A. Karim, SAE Paper 800263, 1980.
13. G. A. Karim, SAE Paper 831196, 1983.
14. G. A. Karim, SAE Paper 88051, 1988.
15. N. Miyamoto, et al., J. Marine Eng. Soc. Japan, 24-3, 1969.
16. R. H. R. Higgins, et al., Int. 12th Symp. on Comb., pp.579, 1969.
17. A. Lifshitz, et al., comb. and Flame, 16-311, 1971.
18. N. Miyamoto, et al., Internal Comb. Engines, 18-224, 1979, Sankaido.